Geomechanics and Engineering, *Vol. 29, No. 3 (2022) 269-279*
https://doi.org/10.12989/gae.2022.29.3.269

Dynamic response evaluation of deep underground structures based on numerical simulation

Mintaek Yoo[**1], Sun Yong Kwon[**2] and Seongwon Hong[*3]

[1]*Railroad Structure Research Team, Korea Railroad Research Institute, Euiwang, 360-1 in Wolam-dong, Uiwang-si, Gyeonggi-do, Republic of Korea*
[2]*Division of Public Infrastructure Assessment, Korea Environment Institute, 370 Sicheong-daero, Sejong-si, Republic of Korea*
[3]*Department of Safety Engineering, Korea National University of Transportation, 50 Daehak-ro, Chungju-si, Chungbuk 27469, Republic of Korea*

(Received December 27, 2021, Revised March 2, 2022, Accepted March 5, 2022)

Abstract. In this research, a series of dynamic numerical analysis were carried out for deep underground building structures under the various earthquake conditions. Dynamic numerical analysis model was developed based on the PLAXIS2D and calibrated with centrifuge test data from Kim *et al*. (2016). The hardening soil model with small strain stiffness (HSSMALL) was adopted for soil constitutive model, and interface elements was employed at the interface between plate and soil elements to simulate dynamic interaction effect. In addition, parametric study was performed for fixed condition and embedded depth. Finally, the dynamic behavior of underground building structure was thoroughly analyzed and evaluated.

Keywords: deep underground building structures; earthquake; HSSMALL; PLAXIS2D; seismic response

1. Introduction

Deep underground structures are significant infrastructure in urban region and extensively utilized as complex shopping malls, building, and even skyscrapers. In Republic of Korea, a number of buildings have had deep underground structures installed and used as commercial facilities and parking lots to overcome shortage of land space. Korean society experienced successive earthquakes of a magnitude exceeding 5.0 in six years, and earthquake (M5.7 2016) in Gyeong-ju city was the largest earthquake ever recorded in Republic of Korea. These events have resulted in great concerns and issues for earthquake stability of major facilities in downtown zone and industrial cities, and seismic design criteria for many facilities have been updated and revised and significance of appropriate design approach for underground structure is strengthened.

Underground structure has been considered as a relatively safe system by seismic behavior (Okamoto 1973). However, it was noted that underground structure also can be extremely damaged or even collapsed during earthquake (Hashash *et al*. 2001, Pitilakis and Tsinidis 2014, Liu *et al*. 2015, Roy and Sarkar 2017). For seismic design, the ground floor is assumed to behave similar with the ground, and the ground factor for ground surface is applied to design the superstructure. However, the deep underground structure such as deep basement parking lot is not included in the structural analysis and design for earthquake. In addition, the amplification of the structure response due to the ground is reduced by the underground structures assumed to be a rigid body without mass (ASCE 2000, FEMA 440 2004, Elsabee and Morray 1977). The motion of the ground, which is a semi-infinite body and actually has mass, could influence the response of the deep underground building structure by occurring an inertial force to the structures. Moreover, the nonlinear boundary condition between the ground and structure must be considered. Despite these conditions, at present, there is no strong consensus in the literature regarding the interaction between the ground and the underground structure.

Liu *et al*. (2018) conducted shake table tests on scaled tunnel model to investigate the mechanism and effect of seismic loadings on horseshoe scaled tunnel model in ground fissure site. In this study, model tunnel exhibited the greatest earth pressure on right and left arches, however, the earth pressure on the crown of arch is the second largest and the inverted arch has the least earth pressure in the same tunnel section. Kwon *et al*. (2020) performed earthquake risk assessment of underground railway station, and showed that moderate or extensive damage could occur the structures constructed in S4 and S5 soil deposit even with return period of 500 years earthquake. Sudevan *et al*. (2020) carried out finite difference modelling to study the liquefaction-induced uplift of an underground structure. Wang *et al*. (2021) investigated the influence of ground motions on the seismic response of utility tunnels. Kwon and Yoo (2021) studied on the dynamic behavior of a vertical tunnel shaft embedded in liquefiable ground, and

∗Corresponding author, Associate Professor
E-mail: shong@ut.ac.kr
**Both authors contributed equally to this manuscript
[a]Senior Researcher
[b]Research Fellow

ISSN: 2005-307X (Print), 2092-6219 (Online)

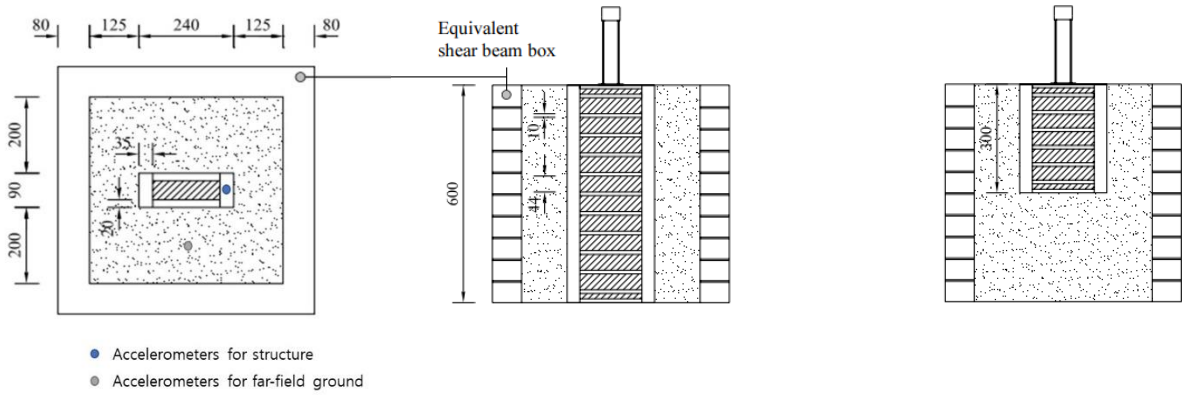

(a) Plan (b) Fixed basement model (c) Half-embedded basement model

Fig. 1 Schematic drawing of test section (unit: mm) (redrawn from Kim *et al*. 2006)

showed that shaft behavior was governed by the soil behavior, which was induced by the kinematic interaction. However, these studies treated underground structure such as tunnel which is located at a certain depth not a deep underground structure which has both the part in contact with the ground surface and the part included in the deep ground.

In this study, a series of dynamic numerical analysis was conducted for deep underground structures for diverse earthquake conditions. Dynamic numerical analysis model was established by using the PLAXIS2D and calibrated based on centrifuge test data from Kim *et al*. (2016). Parametric study was carried out based on embedded depth, embedded condition, and applied seismicity level for eight cases. Each analysis case was set to reflect revised Korean seismic design criteria (Ministry of Interior and Safety 2017).

2. Numerical modeling method and conditions

In this study, seismic responses of deep underground building structure were calculated by PLAXIS2D, which is two-dimensional numerical simulation tools. The numerical model system was simulated based on centrifuge tests from Kim *et al*. (2016) and the analysis results was compared with centrifuge test data for verifying analysis model. The centrifuge tests were conducted at a centrifugal acceleration of 20 g, and the schematic view of the target system is provided in Fig. 1. The structural acceleration was measured by accelerometers attached to the underground structure. Moreover, the far-filed ground acceleration was measured by accelerometers installed in ground surface. The accelerometers for ground surface was installed perpendicular to structure and the direction of shaking to avoid being affected by the structure. The Northridge earthquake with acceleration of 0.16 g was applied to the deep underground building system and shear wave velocity of ground was 194 m/s.

Fig. 2 shows the primary test results of the centrifuge tests. The maximum displacement of fixed basement was 5.31 mm, which is smaller than ground surface displacement of 4.45 mm. The measured displacement of ground surface and underground was in-phase, and the maximum displacement of fixed underground structure without soil was 1.67 mm smaller than that with soil. This kind of phenomenon denotes that the kinematic force by soil was applied to the underground structures as external force. On the other hands, the maximum displacement of half-embedded basement was very similar with that of ground surface. It implies that the soil and structure behave simultaneously. In this study, seismic responses of deep underground building structure observed in centrifuge model tests were calculated by PLAXIS2D. Schematic view of the target system is depicted in Fig. 3. To simulate fixed base condition, bottom section of the soil layer was modeled as rock base condition (green section). Soil and structure models were modeled with prototype scale, and every result obtained from numerical analysis was described with prototype scale as well. In numerical model, dynamic characteristics of soil and structure were considered by applying appropriate material model as follows. Hardening soil model with small strain stiffness (HSSMALL) was adopted for soil constitutive model. This criterion can consider stress dependency of soil shear modulus and hysteretic damping which can simulate nonlinearity of shear modulus and damping ratio as an increase in shear strain was applied. Structure was modelled as elastic and plate element was applied for every part of the structure model. Interface elements were adopted at the interface between plate and soil element to simulate dynamic interaction effect such as strength degradation at interface under earthquake. In the interface element, strength reduction parameter (R_{inter}) which gives a reduced interface friction (wall frictions) and interface cohesion (adhesion) compared to the friction angle and the cohesion in the adjacent soil was employed. In literature review, it is referred that interface friction was somewhat lower than the maximum internal friction of far field and the range of the strength reduction was 60~70% (Kraft *et al*. 1990, Reddy *et al.* 2000). In this study, the average value (0.67) of the range suggested in previous studies was applied with R_{inter} value. Dynamic analysis was then carried out based on 2D plain strain condition and proceeded following steps

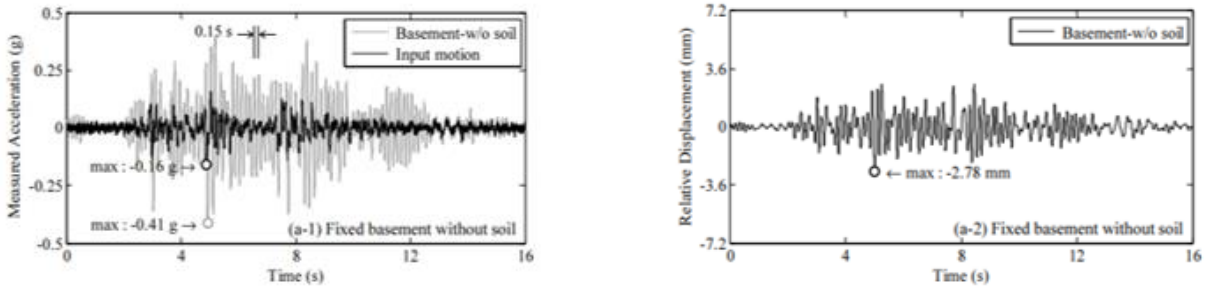

(a) Fixed basement without soil

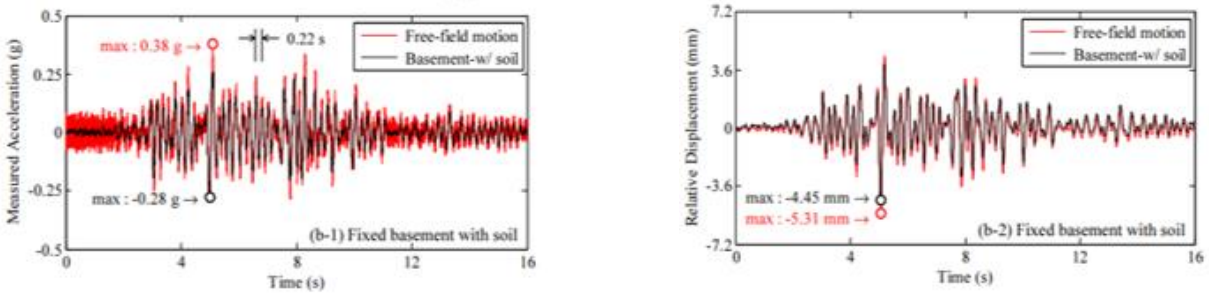

(b) Fixed basement with soil

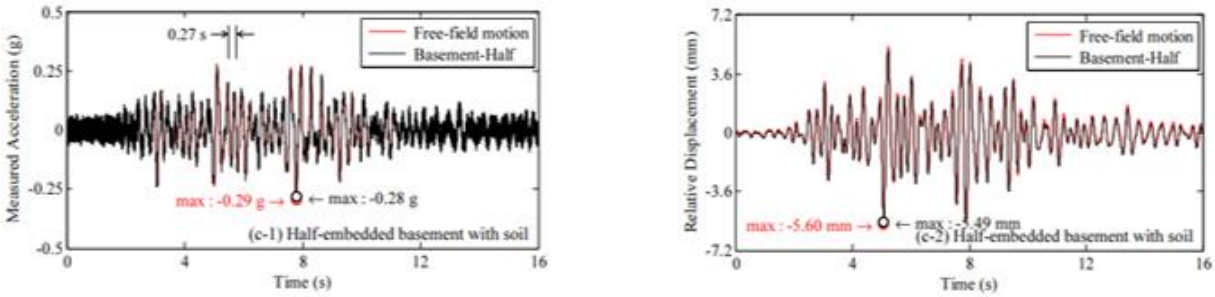

(b) Half-embedded basement with soil

Fig. 2 Time history response of centrifuge tests (Kim *et al*. 2006)

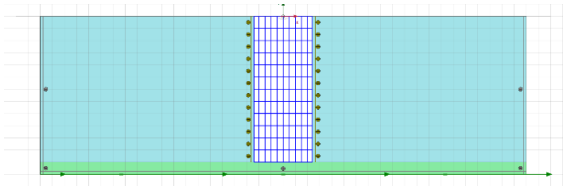

(a) Fixed basement with soil

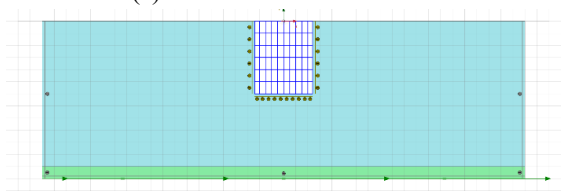

(b) Half-embedded with soil

Fig. 3 Schematic view of the target system calibration case

Table 1 Input properties of model soil and structure

Void ratio	0.5	EI of structure (MPa)	200
Poisson's ratio	0.3	EA of structure (MPa)	12,000
Dry density (kN/m^3)	20	Unit weight of structure (kN/m^3)	25
Friction angle (˚)	30	Cohesion (kN/m^2)	5

according to the construction and loading phases: 1) static equilibrium of soil media, 2) construction of underground building structure and attainment of static equilibrium for overall system, and 3) dynamic analysis. Material properties of the model soil and deep underground building structure are summarized in Table 1. To verify reliability of the numerical model used in this study, calibration of the numerical model with representative experimental results was carried out. For calibration of the numerical model, experimental results of case with Northridge earthquake (input PGA=0.16 g), soil depth of 12 m in 20 gc (refer to Fig. 3) was used.

Figs. 4 and 5 exhibit representative time histories of acceleration and relative displacement obtained in calibration process. Overall trend of seismic responses with time was similar with test results. In the fixed basement with soil, the acceleration fluctuations of the far-field were dominant, whereas in the half-embedded basement with soil the acceleration fluctuations of the structures were dominant. It is considered to be a difference in behavior depending on the fixing conditions at the bottom of the structure, and the same phenomenon was observed in both experiments and analysis results. In the case of relative

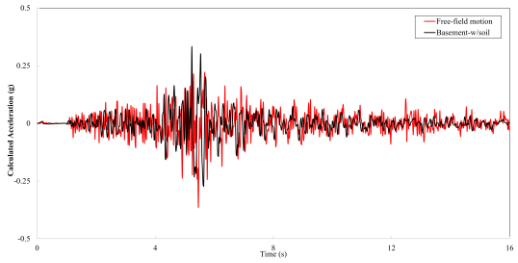

(a) Fixed basement with soil

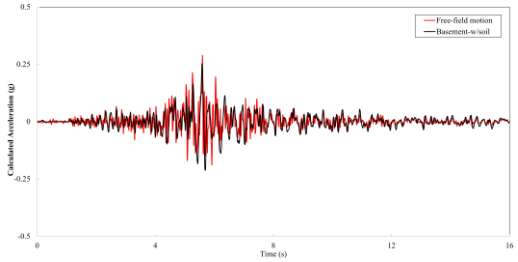

(b) Half-embedded with soil

Fig. 4 Time history response of numerical model (calculated acceleration)

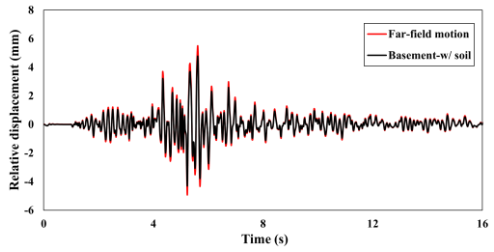

(a) Fixed basement with soil

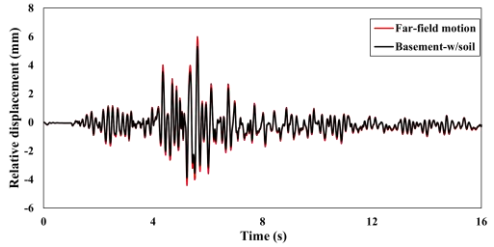

(b) Half-embedded with soil

Fig. 5 Time history response of numerical model (calculated relative displacement)

Table 2 Representative maximum seismic responses calculated from numerical model

	Fixed basement	Half-embedded basement
Maximum acceleration in far-field ground	0.36 g	0.28 g
Maximum acceleration in structure	0.33 g	0.25 g
Maximum relative displacement in far-field ground	0.0054 m	0.0060 m
Maximum relative displacement in structure	0.0047 m	0.0053 m

displacement, while the time history of the far-field and the structure showed in-phase, overall the relative displacement of the far-field showed a larger value than that of the structure. This trend was also found to be the same in both the experimental and analysis results.

Table 2 demonstrates the representative maximum seismic responses calculated from numerical model. It can be confirmed that the numerical model was in good agreement with the experimental results in the case of the maximum values as well as time histories of primary seismic responses. Through a series of calibration procedures, it can be demonstrated that the numerical model used in this study had reliability and applicability.

3. Parametric study using numerical model

Based on the calibration results, parametric study was performed using calibrated numerical model with by thickness of lower normal soil layer, varying analysis conditions. 24 analysis cases were constituted with different thickness of the upper soft soil layer, structure embedded depth, and class of input earthquake motion, as summarized and provided in Table 3 and Fig. 6. Soil layouts were varied with 4 types according to the thickness of soft and normal soil layer. The difference in thickness and Vs (Shear wave velocity of soil deposit) between soft and normal soil layer was established to capture the change in the dramatic seismic behavior of underground structures according to the change in ground conditions. Based on the difference of seismic behavior calculated in underground structure, results of the risk assessment were clearly presented for various model conditions in the following section. Furthermore, ground conditions were constructed to observe the changes in seismic behavior according to the difference in thickness of upper soft soil layer. Similar with the experimental conditions, structure embedded depth simulated the condition fixed to the rock base and the condition floating in the middle of the ground to identify the change in seismic behavior according to the boundary condition at the bottom of the structure. Input earthquake motion in the parametric study was artificially generated from Northridge earthquake and three types of input earthquake motion were determined for parametric study according to the return period (500, 1000, 2400 years) generally applied in Korean seismic design code. These three return periods were determined in order to consider the frequency and intensity of hazard. Input earthquake motions were input at the bottom level of the model in the form of acceleration-time histories. Acceleration-time histories of each earthquake motion used in this study is described in Fig. 7.

Fig. 8 presents relative displacement-time histories calculated in top section of the structure for representative cases among parametric study cases. Cases with fixed base (structure embedded depth of 12 m) show generally larger relative displacement than cases with floated base (structure embedded depth of 6 m). In addition, cases with thicker soft soil layer (V_s=90 m/s) demonstrate relatively larger seismic responses than cases with thinner soft soil layer. These kinds of pattern in seismic response were shown in every case of parametric study. Fig. 9 shows comparisons of

Table 3 List of the analysis cases

Case number	Thickness of soft soil layer(m) (V_s = 90 m/s)	Thickness of normal soil layer(m) (V_s = 360 m/s)	Structure embedded depth(m)	Return period of input motion(year)
1	12	0	12 (Full embedded case)	500
2				1000
3				2400
4	6	6		500
5				1000
6				2400
7	3	9		500
8				1000
9				2400
10	0	12		500
11				1000
12				2400
13	12	0	6 (Half embedded case)	500
14				1000
15				2400
16	6	6		500
17				1000
18				2400
19	3	9		500
20				1000
21				2400
22	0	12		500
23				1000
24				2400

Table 4 Maximum seismic responses for every analysis case

Case number	$ACC_{max,far\text{-}field}$	$ACC_{max,str.}$	$Dis_{max,far\text{-}field}$	$Dis_{max,str.}$
1	0.290 g	0.260 g	0.0094 m	0.0054 m
2	0.384 g	0.349 g	0.0212 m	0.0169 m
3	0.471 g	0.405 g	0.0750 m	0.0679 m
4	0.277 g	0.235 g	0.0040 m	0.0008 m
5	0.367 g	0.336 g	0.0157 m	0.0113 m
6	0.463 g	0.379 g	0.0632 m	0.0589 m
7	0.270 g	0.208 g	0.0027 m	0.0007 m
8	0.349 g	0.316 g	0.0130 m	0.0095 m
9	0.447 g	0.349 g	0.0428 m	0.0370 m
10	0.260 g	0.190 g	0.0010 m	0.0006 m
11	0.316 g	0.266 g	0.0031 m	0.0019 m
12	0.439 g	0.335 g	0.0124 m	0.0098 m
13	0.280 g	0.273 g	0.0100 m	0.0149 m
14	0.374 g	0.351 g	0.0250 m	0.0262 m
15	0.465 g	0.442 g	0.0726 m	0.0719 m
16	0.250 g	0.243 g	0.0032 m	0.0027 m
17	0.346 g	0.341 g	0.0163 m	0.0148 m
18	0.438 g	0.433 g	0.0626 m	0.0632 m

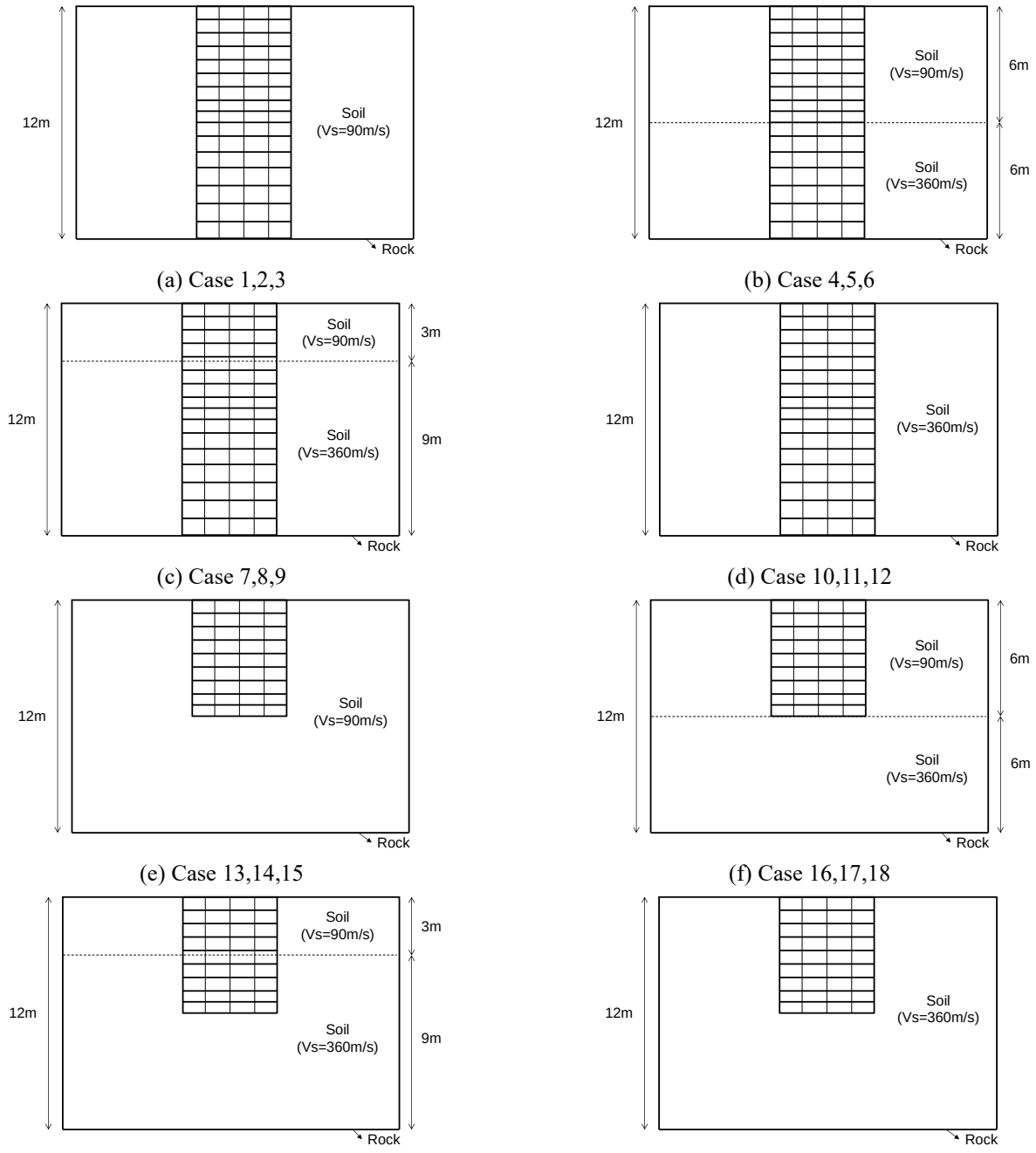

Fig. 6 Schematic view of the analysis cases

acceleration-time histories calculated in far-field ground and structure (top section near ground surface). Far-field ground and structure represented almost in-phase behavior and especially in the case with floated base and peak acceleration value calculated both from far-field ground and structure was almost identical also in the case with floated base. Table 4 provides the maximum seismic responses for every analysis case. The maximum acceleration and relative displacement obtained both from far-field ground and structure (top section near ground surface) generally increased with thickness of the soft soil layer increased and amplitude of input earthquake motion increased. It can be exhibited that site amplification phenomena occurred more in model with thicker soft soil layer than in model with thinner soft soil layer.

4. Discussion

The displacement value obtained from numerical analysis at ground surface and underground structure was analyzed. Figs. 10 and 11 demonstrate the maximum acceleration of ground surface and underground structure with full embedded and half embedded case. When the

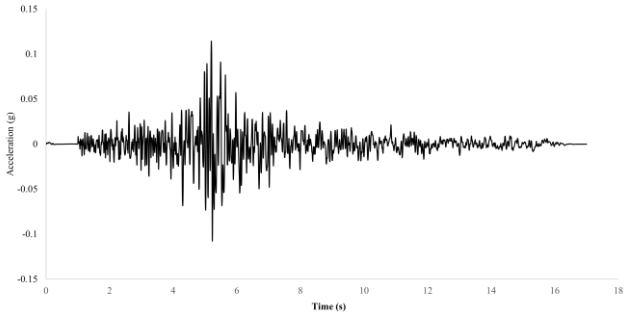

(a) Return period of 500 years

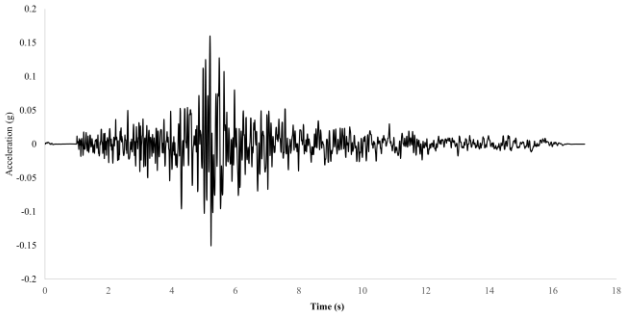

(b) Return period of 1000 years

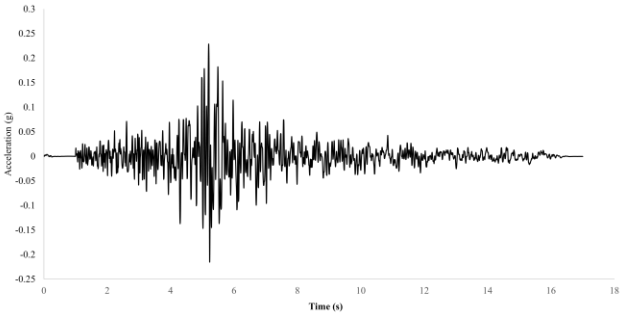

(c) Return period of 2400 years

Fig. 7 Time histories of input earthquake motion (Northridge earthquake)

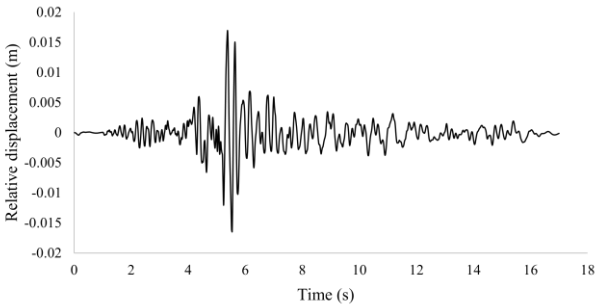

(a) Case No.2

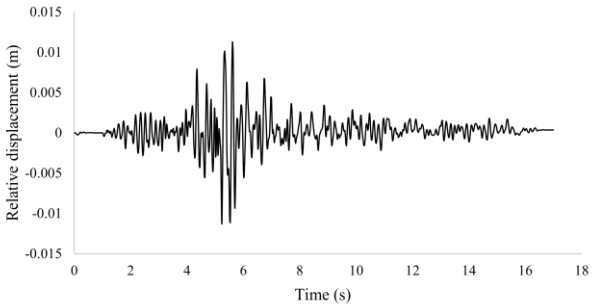

(b) Case No.5

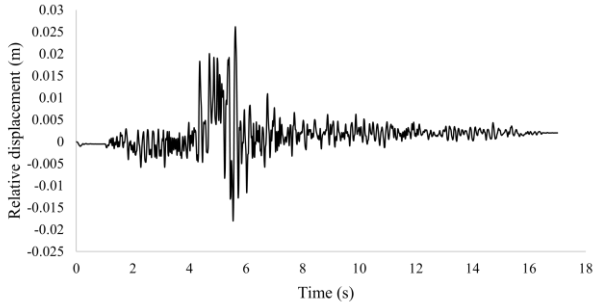

(c) Case No.14

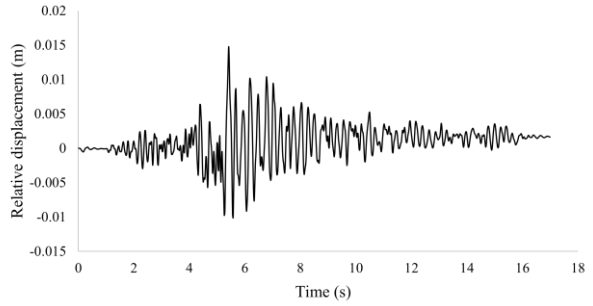

(d) Case No.17

Fig. 8 Relative displacement-time history response of top section of the structure

structure was fixed to bedrock, the structural acceleration was smaller than the ground acceleration due to stiffness difference between ground and structure. On the other hands, when the structure was embedded to the middle part of the ground, the structural acceleration was very similar to the ground acceleration. It means that the structure moved together with the ground.

Fig. 12 shows the acceleration of deep underground structures according to the depth of soft ground. It was observed that as the deep underground building structure was fixed to the bedrock, the effect of the soft ground thickness increased, while the effect decreased as the structure was embedded only to the middle of ground.

The maximum displacement of deep underground for each case is described in Fig. 13. A significantly small lateral displacement of underground structure was observed within 0.5% of the structure width. It implies that the deep underground structures were relatively stable for seismic

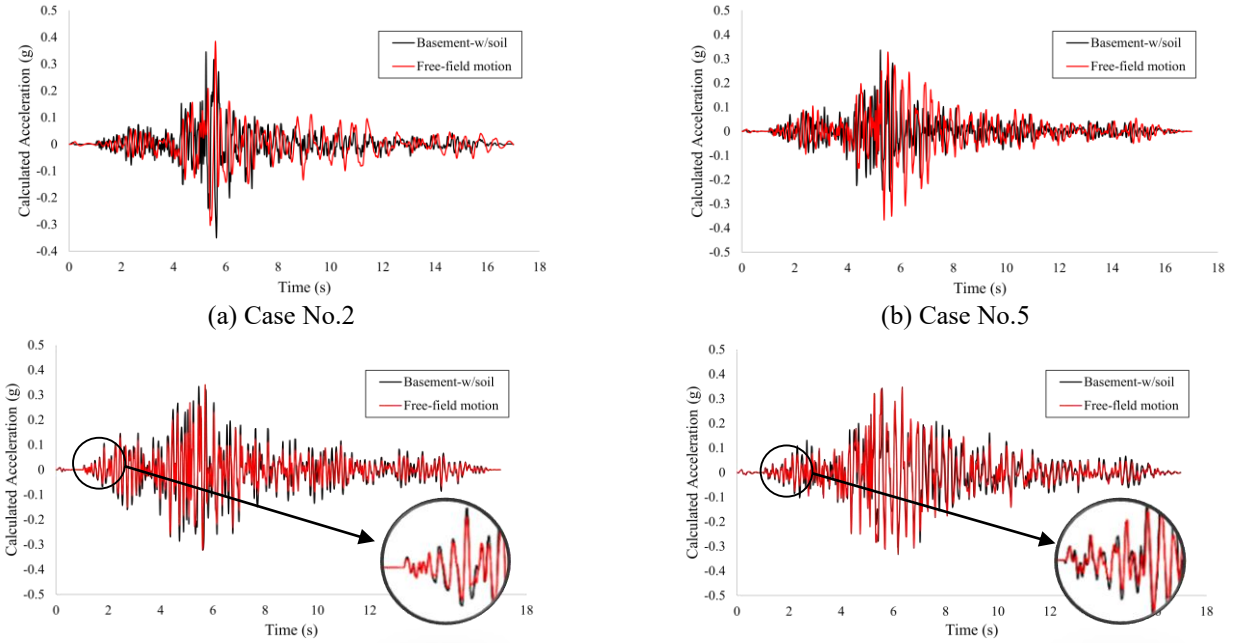

(a) Case No.2 (b) Case No.5

(c) Case No.17 (d) Case No.20

Fig. 9 Acceleration-time history response of far-field ground and structure

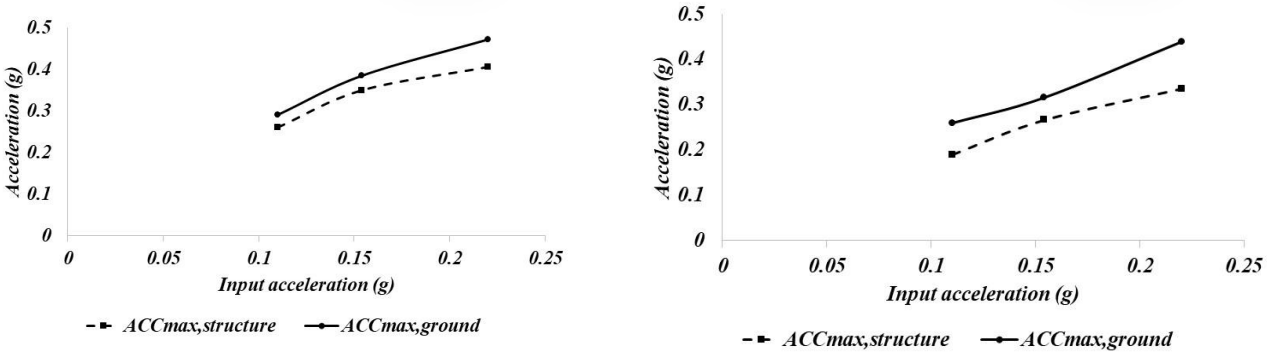

(a) Depth of soft ground layer = 12 m (case 1,2,3) (b) Depth of soft ground layer = 0 m (case 10,11,12)

Fig. 10 Obtained acceleration at ground surface and underground structure (Full embedded structure case)

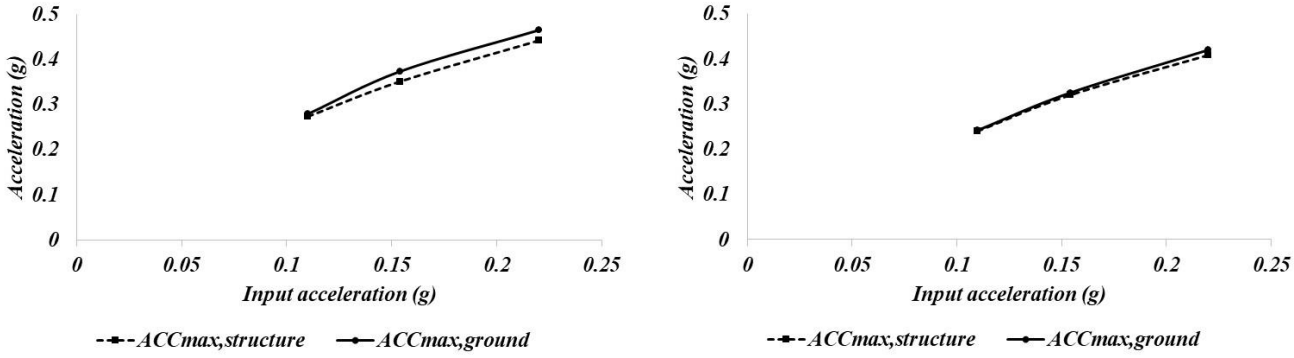

(a) Depth of soft ground layer = 12 m (case 13,14,15) (b) Depth of soft ground layer = 0 m (case 19,20,20)

Fig. 11 Obtained acceleration at ground surface and underground structure (Full embedded structure case)

loading conditions. However, as the thickness of the soft ground layer was large and the structure was not fixed to the bedrock, a relatively large displacement was calculated and there was a displacement beyond the elastic region of

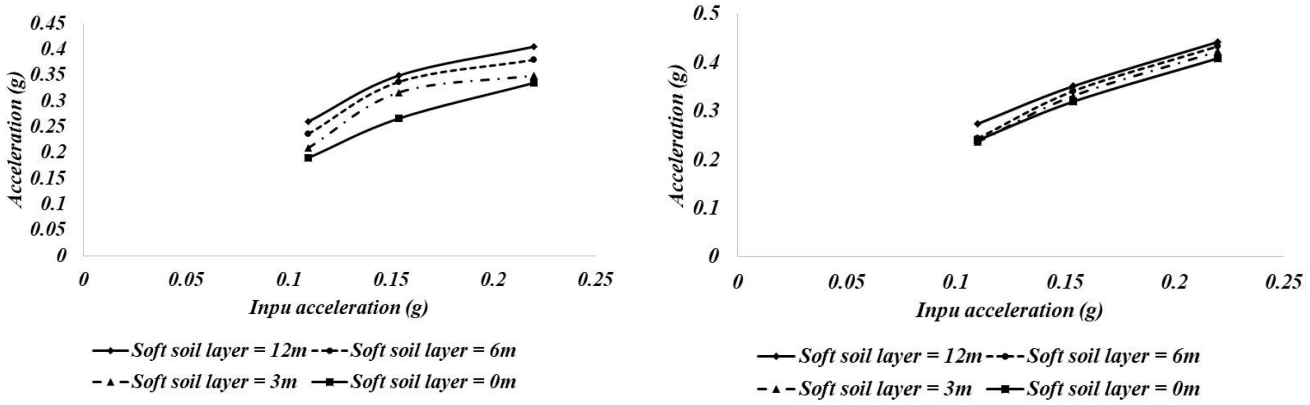

(a) Full embedded case (b) Half embedded case

Fig. 12 Obtained acceleration at underground structure according to soft ground depth

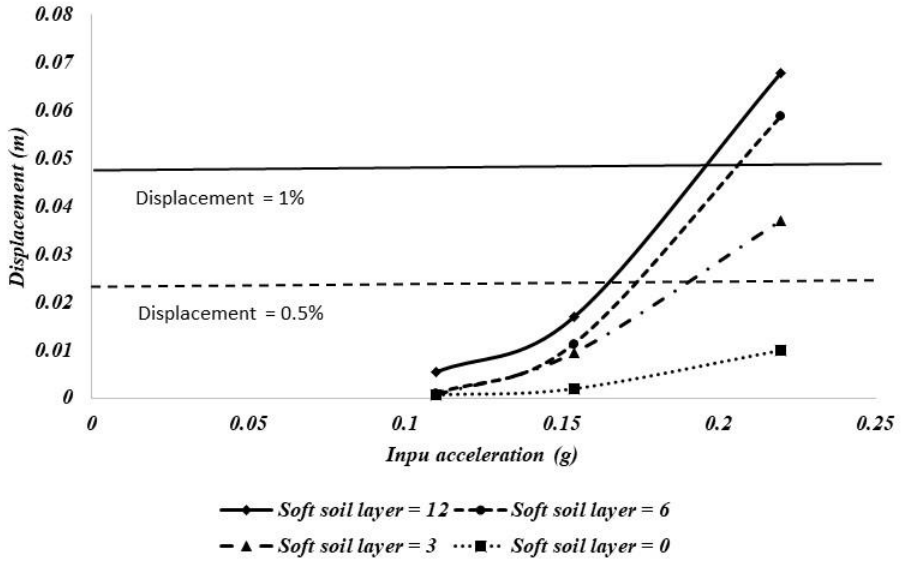

(a) Full embedded case

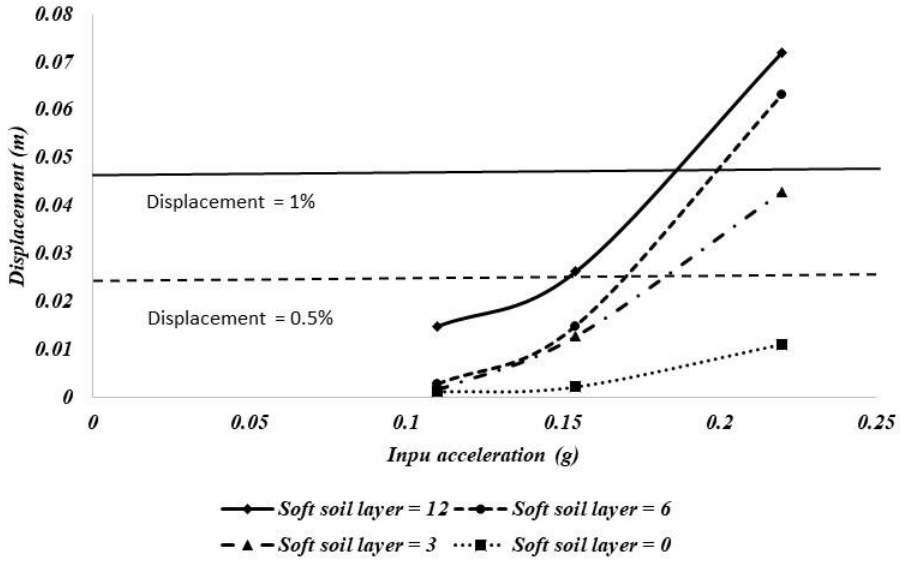

(b) Half embedded case

Fig. 13 Obtained displacement at underground structure according to soft ground depth

Depth of soft ground	12m	6m	3m	0m
500 yrs. of return period	Case 1 None	Case 4 None	Case 7 None	Case 10 None
1000 yrs. of return period	Case 2 None	Case 5 None	Case 8 None	Case 11 None
2400 yrs. of return period	Case 3 Moderate	Case 6 Moderate	Case 9 Minor	Case 12 None

(a) Full embedded case

Depth of soft ground	12m	6m	3m	0m
500 yrs. of return period	Case 13 None	Case 16 None	Case 19 None	Case 22 None
1000 yrs. of return period	Case 14 Minor	Case 17 None	Case 20 None	Case 23 None
2400 yrs. of return period	Case 15 Moderate	Case 18 Moderate	Case 21 Minor	Case 24 None

(b) Half embedded case

Fig. 14 Risk assessment framework based on lateral displacement

Table 5 Damage state

Damage state	Lateral displacement
None	D < 0.5% of structural width
Minor/slight	0.5% of structural width < D < 1% of structural width
Moderate	1% of structural width < DI< 5% of structural width
Extensive	5% of structural width < D

the structure. In case of full embedded case, as the earthquake with return period of 2,400 years occurred on the ground with more than 6m of the soft ground, greater than 1% of width underground structure was measured. In case of half embedded case, the displacement increased compared with the full embedded case, and in soft ground the depth was 12m, the displacement occurred more than 0.5% of the structure width to earthquake with return period of 1,000 years.

Earthquake risk assessment was performed comparing obtained displacement from numerical analysis with width of underground structure. Damage state of deep underground building structures could be classified into three states as minor, moderate and extensive shown in Table 5. To evaluate seismic risk of deep underground structure, the risk assessment frame work was constructed based on damage state analysis results of lateral displacement. The column was the return period of earthquake denoting the hazard intensity. The row was the case number standing for depth of soft ground. In Fig. 14, the risk index indicates higher status with increasing return period earthquake. However, the most severe index was moderate, it signifies that more extensive risk did not occur for deep underground structure in these cases. However, more extensive damage could occur when the depth of soft soil deposit increased. The risk index was riskier with depth of soft ground. The deep underground structure in stiff ground was mostly safe regardless of the hazard intensity.

The risk index was riskier as depth of soft ground increased. The deep underground structure in stiff ground was mostly safe regardless of hazard intensity. As the deep underground structure was constructed on the ground with more than 6m of the soft ground, it could suffer moderate damage by earthquake with return period of 2,400 years. The dynamic centrifuge tests were performed in dry dense sand condition. Therefore, the amplification of seismic loading and ground movement was very small. The numerical analysis model also showed significantly small movement. In these cases, the structure and soil behave with in-phase. Therefore, the further studies for evaluating underground structure in soft ground condition which could occur large ground displacement such as liquefiable ground will be required in future.

5. Conclusions

A series of dynamic numerical analysis were conducted to evaluate seismic behaviors of deep underground building structures. This study has drawn the following detailed conclusions:

- Numerical analysis was carried out to simulate centrifuge model tests performed by Kim *et al*. (2016). In numerical model, dynamic characteristics of soil and structure were simulated by configuring appropriate constitutive model and elements. Calibration of numerical model was conducted by comparing the real seismic responses with the experimental results. The maximum acceleration and relative displacement calculated by numerical model well matched with those observed from centrifuge model tests
- Parametric study was performed using calibrated numerical model with 24 analysis cases which were constituted with thickness of the upper soft soil layer, thickness of lower normal soil layer, structure embedded depth, and class of input earthquake motion. Cases with fixed base show generally smaller relative displacement than cases with floated base. In addition, cases with thicker soft soil layer present relatively larger seismic responses than cases with thinner soft soil layer.
- Far-field ground and structure represented almost in-phase and especially in the case with floated base and peak acceleration value calculated both from far-field and the structure was almost identical also in the case with floated base. Peak acceleration and relative displacement obtained both from far-field and structure generally increased with thickness of the soft soil layer increased and amplitude of input motion increased. It can be exhibited that site amplification phenomena occurred more in model with thicker soft soil layer than in model with thinner soft soil layer.
- To evaluate seismic risk of deep underground structure, risk assessment frame work was constructed based on damage state analysis results of lateral displacement. Based on the results, it was concluded that minor and moderate damage could occur on the deep underground structure constructed ground with more than 6m of the soft ground.

Acknowledgments

This research was supported by a grant (KAIA22SCIP-C155167-04) from Construction Technologies Program funded by Ministry of Land, Infrastructure and Transport of Korean government, Korea Environment Industry & Technology Institute (KEITI) funded by the Korea Ministry of Environment(MOE) (2020002990007), Decision Support System Development Project for Environmental Impact Assessment Project, 2022-003(R)) funded by Korea Environment Institute(KEI), and and the Young Researcher Program through the National Research Foundation of Korea (NRF) funded by the Korea government (MSIT; Ministry of Science and ICT) (2021R1C1C1010087).

References

ASCE (2000), "Seismic analysis of safety related nuclear structures and commentary", *Am. Soc. Civ. Eng.*, 4-98.

Elsabee, F. and Morray, J.P. (1977), "Dynamic behavior of embedded foundations", Rpt. No. R77-33, MIT.

FEMA 440 (2004), *Improvement of Nonlinear static seismic analysis procedures*, Federal Emergency Management Agency, Washington DC, USA.

Hashash, Y.M., Hook, J.J., Schmidt, B., John, I. and Yao, C. (2001), "Seismic design and analysis of underground structures", *Tunn. Undergr. Sp. Tech.*, **16**(4), 247-293. https://www.sciencedirect.com/science/article/pii/S0886779801000517.

Kim, D.K., Park, H.G., Kim, D.S. and Ha, J.G. (2016), "Centrifuge Test for Earthquake Response of Structures with Basements", *J, Earthq. Eng, Soc. Korea*, **20**(4), 223-234. https://doi.org/10.5000/EESK.2016.20.4.223.

Kraft Jr, L. M. (1990), "Computing axial pile capacity in sands for offshore conditions", *Mar. Geores. Geotech.*, **9**(1), 61-92.

Kwon, S.Y., Yoo, M. and Hong, S.W. (2020), "Earthquake risk assessment of underground railway station by fragility analysis based on numerical simulation", *Geomech. Eng.*, **21**(2), 143-152. https://doi.org/10.12989/gae.2020.21.2.143.

Kwon, S.Y. and Yoo, M. (2021), "A study on the dynamic behavior of a vertical tunnel shaft embedded in liquefiable ground during earthquakes", *Appl. Sci.*, **11**(4), 1560. https://doi.org/10.3390/app11041560.

Liu, X.R., Li, D.L., Wang, J.B. and Wang, Z. (2015), "Surrounding rock pressure of shallow-buried bilateral bias tunnels under earthquake", *Geomech. Eng.*, **9**(4), 427-445. https://doi.org/10.12989/gae.2015.9.4.427.

Liu, N., Huang, Q.B., Fan, W., Ma, Y.J. and Peng, J. B. (2018), "Seismic responses of a metro tunnel in a ground fissure site", *Geomech. Eng.*, **15**(2), 775-781. https://doi.org/10.12989/gae.2018.15.2.775.

Ministry of Interior and Safety (2017), "*Common Application of Seismic Design Criteria*", Sejong, 4.

Okamoto, S. (1973), Introduction to earthquake engineering, University of Tokyo Press, Tokyo, 29-40.

Pitilakis, K. and Tsinidis, G. (2014), *Performance and Seismic Design of Underground Structures*, Springer International Publishing, New York, NY, USA.

Reddy, E.S., Chapman, D.N. and Sastry, V.V. (2000), "Direct shear interface test for shaft capacity of piles in sand", *Geotech. Test. J.*, **23**(2).

Roy, N. and Sarkar, R. (2017), "A review of seismic damage of mountain tunnels and probable failure mechanisms", *Geotech. Geol. Eng.*, **35**(1), 1-28. https://link.springer.com/article/10.1007/s10706-016-0091-x.

Sudevan, P.B., Boominathan, A. and Banerjee, S. (2020), "Mitigation of liquefaction-induced uplift of underground structures by soil replacement methods", *Geomech. Eng.*, **23**(4), 365-379. https://doi.org/10.12989/gae.2020.23.4.365.

Wang, C., Ding, X., Chen, Z., Feng, L. and Han, L. (2021), "Seismic response of utility tunnels subjected to different earthquake excitations", *Geomech. Eng.*, **24**(1), 67-79. https://doi.org/10.12989/gae.2021.24.1.067.